# *Loss of spatial organization and destruction of the pericellular matrix in early osteoarthritis in vivo and in a novel in vitro methodology*

HHS Public Access

Author manuscript

*Osteoarthritis Cartilage*. Author manuscript; available in PMC 2017 July 01.

Published in final edited form as:

*Osteoarthritis Cartilage*. 2016 July ; 24(7): 1200–1209. doi:10.1016/j.joca.2016.02.001.

# Loss of spatial organization and destruction of the pericellular matrix in early osteoarthritis *in vivo* and in a novel *in vitro* methodology

**Tino Felka**[1], **Miriam Rothdiener**[1], **Sina Bast**[1], **Tatiana Uynuk-Ool**[1], **Sabra Zouhair**[2], **Björn Gunnar Ochs**[3], **Peter De Zwart**[3], **Ulrich Stoeckle**[3], **Wilhelm K Aicher**[4], **Melanie L Hart**[4], **Thomas Shiozawa**[5], **Alan J Grodzinsky**[6], **Katja Schenke-Layland**[7,8], **Jagadeesh K Venkatesan**[9], **Magali Cucchiarini**[9], **Henning Madry**[9], **Bodo Kurz**[10], and **Bernd Rolauffs**[1,3,6,*]

[1]Siegfried Weller Institute for Trauma Research, BG Trauma Clinic Tuebingen, University of Tuebingen, Tuebingen, Germany

[2]Department of Cardiac, Thoracic and Vascular Sciences, University of Padua, Padua, Italy

[3]Clinic for Trauma and Restorative Surgery, BG Trauma Clinic Tuebingen, University of Tuebingen, Tuebingen, Germany

[4]Department of Urology, University of Tuebingen, Tuebingen, Germany

[5]Institute of Clinical Anatomy and Cell Analysis, University of Tuebingen, Tuebingen, Germany

[6]Center for Biomedical Engineering, Massachusetts Institute of Technology, Cambridge, USA

[7]Department of Women's Health, Research Institute for Women's Health, University of Tuebingen, Tuebingen, Germany

[8]Department of Cell and Tissue Engineering, Fraunhofer Institute for Interfacial Engineering and Biotechnology (IGB), Stuttgart, Germany

[*]Corresponding Author: Bernd Rolauffs, Siegfried Weller Institute for Trauma Research, BG Trauma Clinic Tuebingen, University of Tuebingen, ZMF, Waldhoernlestr. 22, 72074 Tuebingen, Germany, berndrolauffs@googlemail.com.



**COMPETING INTERESTS**

The authors declare that they have no conflict of interest.

**AUTHOR CONTRIBUTIONS**

T.F. prepared adult OA cartilage samples, conducted their immunofluorescence analyses and analyzed the adult pericellular matrix histologically. M.R. helped assessing the pericellular matrix of chondrocytes and the FGF-2 experiments. S.B. analyzed adult cartilages after gene transfer of plasmids and rAAV vectors via immunofluorescence analyses, and performed immunofluorescence analyses of samples prior to scanning electron microscopy. T.U.-O. helped digitally recording the chondrocytes within their tissue. S.Z. prepared fetal cartilage samples, and conducted immunofluorescence analyses of the fetal pericellular matrix. B.G.O., P.D.Z. and U.S. contributed with acquiring and grading the human materials used, and they critically discussed and improved the manuscript. W.K.A. and M.L.H. helped with data analysis, interpretation and discussion. A.J.G helped interpreting and discussing the data and provided his expertise on OA pathology. K.S.L. performed multiphoton imaging and analysis. J.K.V., M.C., and H.M. prepared adult cartilage samples and performed gene transfer of plasmids and rAAV vectors. B.K. performed scanning electron microscopy, helped discussing and interpreting the acquired data and underlying hypotheses, and helped improving the manuscript. B.R. conceived and designed this study, its hypotheses and experiments, acquired the funding necessary to conduct this study, served as study coordinator, and prepared the adult intact cartilage samples from human donors. He interpreted and merged the data acquired in the involved laboratories into its present form, performed the statistical analyses, and wrote the manuscript.

[9]Center of Experimental Orthopaedics, Saarland University Medical Center, Homburg, Germany

[10]Anatomical Institute, Christian-Albrecht-University Kiel, Kiel, Germany

## Abstract

**Objectives—**Current repair procedures for articular cartilage cannot restore the tissue's original form and function because neither changes in its architectural blueprint throughout life nor the respective biological understanding is fully available. We asked whether two unique elements of human cartilage architecture, the chondrocyte-surrounding pericellular matrix (PCM) and the superficial chondrocyte spatial organization (SCSO) beneath the articular surface are congenital, stable or dynamic throughout life. We hypothesized that inducing chondrocyte proliferation *in vitro* impairs organization and PCM and induces an advanced OA-like structural phenotype of human cartilage.

**Methods—**We recorded propidium-iodine-stained fetal and adult cartilage explants, arranged stages of organization into a sequence, and created a lifetime-summarizing SCSO model. To replicate the OA-associated dynamics revealed by our model, and to test our hypothesis, we transduced specifically early OA-explants with hFGF-2 for inducing proliferation. The PCM was examined using immuno- and auto-fluorescence, multiphoton second-harmonic-generation, and scanning electron microscopy.

**Results—**Spatial organization evolved from fetal homogeneity, peaked with adult string-like arrangements, but was completely lost in OA. Loss of organization included PCM perforation (local micro-fibrillar collagen intensity decrease) and destruction (regional collagen type VI signal weakness or absence). Importantly, both loss of organization and PCM destruction were successfully recapitulated in FGF-2-transduced explants.

**Conclusion—**Induced proliferation of spatially characterized early OA-chondrocytes within standardized explants recapitulated the full range of loss of SCSO and PCM destruction, introducing a novel *in vitro* methodology. This methodology induces a structural phenotype of human cartilage that is similar to advanced OA and potentially of significance and utility.

### Keywords

articular cartilage; chondrocyte; superficial zone; cartilage architecture; spatial organization; cellular distribution; early osteoarthritis; early OA; pericellular matrix; PCM; multiphoton imaging

---

Articular cartilage (AC) is a weight-bearing tissue with a specialized architecture that the sole resident cells, the chondrocytes, build and maintain. However, they attempt but fail to successfully repair the tissue once damaged. To delay or avoid the progression of osteoarthritis (OA), a major debilitating disease, current therapies replace the tissue or surgically induce the migration of regeneration-competent cells from the subchondral bone[1]. None of the procedures re-create the original tissue function[2] or architecture[3], highlighting that developing more sufficient treatment strategies is hindered by a limited understanding of basic cartilage biology.

Major OA events occur at the level of chondrocytes[4], specifically at the articular surface[5] in areas where mechanical forces are greatest[6]. Here, proliferative chondrocyte clones

form early in the disease[7, 8] at the margins of fibrillation[9] as a hallmark of OA[10]. These clones express a range of activation and abnormal differentiation markers[7] and sustain the activation of molecular pathways of inflammatory signal transduction[4]. However, research aimed at establishing a unified theory of the initial OA dysfunction was so far not successful[11]. Better recognition and understanding of pre-osteoarthritic disease states will be critical for developing effective strategies for treating and, ultimately, preventing early OA[4, 10].

Recent advancements identified specific chondrocyte arrangements ("superficial chondrocyte spatial organization"; SCSO) as a significant characteristic of AC architecture[12]. Beneath the intact joint surface, superficial chondrocytes are arranged in four basic spatial patterns: strings, clusters, pairs and single cells[13]. Each joint surface is dominated by one of those patterns[13]. The resulting SCSO display high levels of complexity[14] and are species-, joint type- and surface-specific[12], much like biological fingerprints. Changes in the SCSO specifically associated with early OA can be utilized for early preclinical disease detection[12, 15], emphasizing the importance of this architectural characteristic. However, despite this knowledge[12–16], little is known about the dynamic nature of the SCSO. Here, we asked whether the SCSO is congenital, stable or dynamic throughout life. First, we created a SCSO model that summarizes the lifetime of a hypothetical human individual, based on arranging specific stages into a sequential order. We based the fetal sequence of specific stages on the week of gestation and the adult OA-related sequence on the hypothesis that chondrocyte proliferation is a major mechanism capable of inducing SCSO changes. The rationale was that proliferation occurs transiently in early OA and is responsible for chondrocyte clone formation[7, 8]. We aimed to recapitulate OA-related changes in the SCSO *in vitro* by inducing proliferation specifically within early OA cartilage (identified using SCSO characteristics aberrant from healthy tissues as an indicator for early OA)[12]. The successful recapitulation of OA-related changes in the SCSO would confirm our main hypothesis and also the soundness of our lifetime-summarizing model. Additionally, re-creating SCSO impairment *in vitro* would introduce the opportunity to study relevant aspects of early OA progression over time and in the sense of a novel *in vitro* methodology. Finally, SCSO changes may potentially affect the structural vicinity of the chondrocyte. Thus, we focused on the chondrocyte-surrounding pericellular matrix (PCM), which has protective[17], regulatory and mechano-transduction functions[18, 19]. Linking early OA SCSO changes to proliferation and PCM impairment would broaden our understanding of basic cartilage biology.

## METHODS

### Human articular cartilages

Human fetal lower extremities were obtained during medical abortion and human fetal knee joints from still births. Fetal serial cryosections (100μm) were prepared perpendicular to the longitudinal axis of the lower extremity. Condylar cartilage sections were selected. Location-matched cartilages were obtained from cadaveric condyles of healthy human donors, and of patients diagnosed with clinical OA prior to knee replacement. Each articular surface (AS) was graded with a 5-point scale established by Collins-Muehleman[16]. All tissues were

obtained with approval of the local research ethics committee and informed consent (fetal cartilage: 710/2012BO1; intact cartilage: 452/2010BO1; OA: 171/2014BO2). The aim was to obtain comparable numbers of cartilage samples across the conditions analyzed.

## Fluorescence-microscopy

**Spatial organization—**Fetal cartilage cryosections and adult cartilages (uncut joint surface; sample size approx. 1cm$^2$) were stained with propidium iodide (P.I., Sigma) as described[13, 15, 16], washed with 1% Triton X-100 (Sigma) in phosphate-buffered saline (PBS; PAA) for 5min, stained for 60min with P.I. (10 μg/ml in PBS), and washed for 10min with Tris-buffered saline (0.1M Tris, 0.15M NaCl, pH 7.5). All samples were viewed in a top-down view onto the articular surface. Z-stacks were digitally recorded (Zeiss LSM510, AxioVison4.8, 1μm slice distance, 1388×1040px) with ApoTome starting beneath the surface when chondrocytes first came into focus and stopping when the P.I. signal intensity was too low for capture. The top-most chondrocytes were further analyzed. Color-coded local cell density maps were calculated[15].

**PCM—**Serial cryosections (50 μm) of the adult superficial zone were prepared parallel to the condylar surface (n=6 patients; 66–74 years), washed in PBS, fixed with 4% paraformaldehyde (Merck), incubated with primary monoclonal antibodies (goat anti-Collagen6A3, Santa Cruz. 1:50 dilution) overnight, washed, and incubated with secondary antibody (donkey anti-goat FITC-conjugated, Santa Cruz, 1:100 dilution). Chondrocyte nuclei were stained with DAPI (Sigma). PCM was visualized in a top-down view onto the AS as described[13, 15, 16] (LSM510). Negative controls were incubated with COL6A3 blocking peptide (Santa Cruz, 1:50 dilution) prior to anti-COL6A3 antibody incubation or without primary antibodies.

## Distinct stages & model of the spatial organization

Chondrocyte groups were defined as chondrocytes in proximity of each other forming distinct spatial patterns[13]. The recorded z-stacks were visually classified according to their dominant pattern of SCSO such as chondrocyte strings, clusters, pairs or single chondrocytes, as observed in intact cartilage[13], chondrocyte double strings as observed in the macroscopically intact cartilage of joints with focal OA[16], and the absence of any discernible organization based on randomly aggregating cells within OA-lesions, termed “diffuse” arrangement[15]. For fetal cartilages, the sequential order of the spatial stages was determined by the week of gestation. For adult cartilages, the number of cells per chondrocyte group was determined for randomly chosen chondrocyte groups from all images that represented the adult spatial stages (e.g. the number of chondrocytes per string was determined for images classified as string stages). The adult spatial stages were sequentially ordered by an increasing average cell number per group. This sorting approach from smaller to larger cell numbers per chondrocyte group was based on the below tested and confirmed hypothesis that chondrocyte proliferation is the mechanism of SCSO changes. Recorded z-stacks were also used for calculating the 3D-Cartesian coordinates of the chondrocyte nuclei (AxioVision4-Module 3D-measurement). Based on these coordinates, the Clark-Evans-Aggregation-Index (R) was calculated to assess whether the

spatial cellular arrangement was random, homogeneous or grouped, as described[13, 15, 16].

## Gene transfer of plasmids and rAAV vectors

Chondrocyte proliferation was induced specifically in early OA cartilage, represented by explants containing chondrocyte double strings confirmed for selected samples[16]. Samples were taken from the macroscopically most intact areas of the condylar joint surface of patients undergoing knee joint replacement (n=6 patients; 45–76 years). Chondrocyte transduction used rAAV-hFGF-2 and rAAV-RFP as a control. rAAV-hFGF-2 carries a 480-bp hFGF-2 cDNA fragment[20] that was cloned in rAAV-lacZ in place of lacZ[21]. rAAVlacZ is an AAV-2-based plasmid carrying the lacZ gene encoding beta-galactosidase (b-gal) under control of the cytomegalovirus immediate-early (CMV-IE) promoter[22]. rAAV-RFP carries a Discosoma sp. red fluorescent protein (RFP) cDNA (776 bp)[23]. rAAV vectors were packaged as single-stranded elements using Adenovirus 5 to provide helper functions in combination with pAd8[21, 22]. pAd8 contains AAV-2 replication and encapsidation functions[24]. Vector preparations were purified by dialysis and titrated by RT-PCR (1010 functional units/ml). The vectors were provided to the cartilage disks based on concentrations previously tested[22]. Disks were transduced (20 or 50 μl) or co-transduced (20 μl each vector) by direct rAAV application to the surface for 2 days[21, 22]. Efficacy of the rAAV-mediated gene transfer in situ was monitored by detecting either β-gal activities based on rAAV-lacZ gene transfer (X-Gal staining and evaluation of the % stained cells under light microscopy) or live fluorescence based on rAAV-RFP gene transfer (evaluation of % fluorescent cells under confocal microscopy)[21–23]. The samples were incubated for 28 days. Subsequently, SCSO and cell numbers were further analyzed.

## Multiphoton-induced autofluorescence and second-harmonic-generation (SHG) imaging

Multiphoton-induced autofluorescence was used to localize fetal chondrocytes within the cryosections and adult strings and clusters within the joint surface of non-processed, live cartilage samples (n=3 patients; 65–73 years). The chondrocyte PCM was analyzed by SHG imaging [25]. Micro-fibrillar collagen components of the PCM were non-destructively analyzed at two different laser excitation wavelengths. Exposure to laser pulses at 740nm revealed autofluorescent chondrocytes, whereas imaging of the same intra-tissue regions at 840nm revealed fibrous collagen structures. Due to femtosecond laser-induced SHG processes, emitted blue light at a peak emission wavelength of 420nm served as a quantitative measure of the micro-fibrillar collagen PCM content. SHG radiation was achieved using a filter FB420-10 (Thorlabs) in front of the detector. A 700nm short-pass-filter (E700SP, Chroma Technology) prevented scattered laser radiation blocking UV radiation (transmission range: 390–700nm). To quantify the intrinsic fluorescence signals of collagenous structures, lambda stacks were ascertained at emission wavelengths of 390–490nm (in 10nm increments) using Chameleon laser (Coherent Laser Group) tuned to an 840nm excitation wavelength. Emission was collected using the Zeiss META detector of the LSM 510 Meta NLO system (Carl Zeiss MicroImaging). The scans were acquired with a scan time of 2.561s/pixel, eight times summarization to enhance the signal, in plane multi track 8-bit lambda mode, and analyzed by AIM3.2 software (Zeiss). SHG signal intensities were reflected by the grey values of all pixels and were comparable across all images due to

a reproducible laser excitation power and similar exposure times. The mean gray value intensities were calculated to represent the micro-fibrillar collagen intensity.

### Scanning electron microscopy (SEM)

Condylar cartilage samples were fixed in 3% glutaraldehyde/PBS overnight, fixed for 60min with 2% osmium ($OSO_4$; Pasel und Lorei GmbH), dehydrated in ethanol, dried (Balzers, Critical point dryer 030), mounted, sputter coated with gold (Ion Tech LTD), and digitally recorded (Phillips XL20SE microscope).

### Statistical analyses

All data are presented as mean±95% confidence intervals. Calculations were performed with Microsoft Excel2010 and SigmaPlot-11.0.0.77 (Systat). Data were analyzed for normality (Kolmogorov-Smirnov-test). Normally distributed data were subjected to the Student's t-test; non-normal data to the Mann-Whitney-Rank-Sum-Test. More than two groups were compared using ANOVA and post-hoc tests. Differences were considered statistically significant at $p<0.05$.

## RESULTS

### SCSO model

Location-matched cartilages of 4 adult donors (ages 43–64 years; gender ratio: 1:1, Collins grade: 0) and 6 OA patients (ages 60–75 years, gender ratio: 1:1; Collins grade: 3) were included. Fetal cartilage availability was limited. Tissues from the 8th (n=3) and the 21st, 33rd, 39th, and 40th weeks of gestation (n=1 each) were included. Chondrocytes illustrated a range of different cellular arrangements. Each image was classified according to its predominant spatial pattern. To organize these classified arrangements into one sequence, the fetal stages were arranged based on an increasing week of gestation, and the adult stages were arranged based on an increasing number of chondrocytes per cell group (strings: 4.94±0.71 cells, double strings: 7.40±0.77, small clusters: 19.46±2.79, large clusters: 73.77±5.78; diffuse arrangement: 541.33±183.47; diffuse: n=6 images, n=35 cell groups for each stage). A small image subset was characterized by low cellularity and absent organization, and the number of cells per chondrocyte group could not be determined due to the absence of cell groups. These images were classified as end-stage OA because hypocellularity is a criterion of a high Mankin score and end-stage OA is associated with loss of organization [12]. To illustrate the resulting sequence of the specific stages of SCSO, representative stages were assembled into a model (Fig. 1), which summarized the changes that occur during the lifetime of a hypothetical individual. Only the spatial stages illustrated in Fig. 1 were observed.

The model revealed that at weeks 8–39 of gestation, fetal chondrocytes showed no specific organization or cell groups typical for adult chondrocytes. At week 40, chondrocytes were situated in groups that begun to resemble the typical adult string pattern. The peak of organization were chondrocyte strings, typical for healthy cartilage as demonstrated[13]. With OA onset, chondrocytes were predominantly arranged in double strings. With increasing chondrocyte numbers per cell group, double strings were surpassed by small and

large chondrocyte clusters. Next, a diffuse arrangement without any recognizable organization appeared as one large cell group spread out across the entire image region. The final stage consisted of areas with a low number of chondrocytes and the absence of cell groups and recognizable organization. Thus, our model revealed that the SCSO of human joint surfaces is not inborn, but matures with time around week 40. The SCSO peaks in the healthy adult with chondrocytes strings and undergoes complete destruction with OA.

### Recapitulating loss of spatial organization within cartilage

To recapitulate SCSO loss in OA, and to experimentally test our proliferation hypothesis, proliferation was induced by FGF-2-transduction specifically in string and double string chondrocytes of early OA cartilage. In controls, 28 days after rAAV-RFP-transduction, the SCSO remained as strings and double strings (Fig. 2A). However, those were not recognizable in rAAV-FGF-2-transduced cartilages, where the organization was severely altered (Fig. 2B), comparable to the diffuse model stage (Fig. 1). In rAAV-FGF-2 explants, chondrocyte numbers were 2.13-fold higher vs. controls (FGF-2: 664±100 chondrocytes/ $900\times650\mu m^2$ joint surface, RFP: 287±81, $p<0.05$) demonstrating proliferation. Proliferation led to a significantly increased local cell density within the AS(Fig. 2A,B) and an increased chondrocyte number per normalized area (Fig. 2D). Thus, starting specifically with early OA cartilage, the cellular organization transitioned from strings/double strings into a diffuse arrangement lacking any discernable organization. Effectively, we have recapitulated SCSO loss, suggesting that chondrocyte proliferation may be a mechanism responsible for OA-associated SCSO changes.

### Impairment of the PCM structure

The fluorescent collagen type VI (CollVI) signal, a major PCM component, beneath the ASwas low within fetal surfaces, but strong in adult intact surfaces (Fig. 3). OA-joint surfaces with chondrocyte clusters contained little or no detectable CollVI. Areas without discernible organization were characterized by signal absence (Fig. 3). Using multiphoton-induced autofluorescence microscopy, we localized fetal and adult chondrocytes of interest (Fig. 4A). Performing SHG microscopy on these groups (Fig. 4B), the micro-fibrillar collagen intensity of fetal cartilage was near zero and significantly lower than that of the PCM surrounding chondrocyte strings (4.7±0.8 vs. 156.7±12.4, $p<0.001$, Fig. 4C). Compared to string chondrocytes, clusters had a 0.48-fold lower collagen intensity (74.9±6.7, $p<0.001$, Fig. 4C). Thus, fetal chondrocytes were not surrounded by a collagenous PCM. The intact adult PCM was characterized by the abundant presence of micro-fibrillar collagens whereas the PCM surrounding OA-chondrocyte clusters was structurally compromised in its micro-fibrillar collagen content. Additionally, we recorded individual chondrocytes exiting or being released from the PCM using immunofluorescence microscopy (Fig. 5A). In support of these observations, SHG signals revealed clearly demarcated PCM perforations with a low micro-fibrillar collagen intensity (18.0±3.1) compared to intact parts of the same PCM (104.2±5.4, $p<0.001$, Fig. 5B, C). SEM of the PCM of the topmost chondrocytes revealed *ex vivo* a network of interwoven fibers surrounding chondrocyte strings. This network was less apparent around clustered chondrocytes. The cell-matrix interface was irregularly shaped and broken up, suggesting a structurally compromised, partially absent PCM of clustered chondrocytes (Fig. 6A). Thus,

our data collectively suggested that chondrocytes undergoing loss of SCSO beneath the joint surface were surrounded by a structurally impaired PCM, including an absence of the major PCM component CollVI in diffusely arranged chondrocytes, a significant decrease of micro-fibrillar collagens, and an irregularly shaped, broken up cell-matrix interface. Individual chondrocytes exiting or being released from their PCM appeared to be related to this impairment through clearly demarcated PCM perforations with low micro-fibrillar collagen intensity.

### Recapitulating OA-associated structural PCM impairment within cartilage

We performed SEM on cartilage explants, in which SCSO loss was successfully re-capitulated through induced proliferation. 28 days after FGF-2 transduction, SEM revealed an irregularly shaped, broken up, and partially absent PCM (Fig. 6B). In controls, which had maintained their SCSO, chondrocyte strings were surrounded by an intact PCM. Thus, induced proliferation correlated with an impaired structural integrity of the PCM, in addition to SCSO loss (demonstrated above). Hence, the processes of PCM impairment and SCSO loss were intertwined.

### Quantitative analyses of the distinct stages of the spatial organization

The Clark-Evans-Aggregation-Index as a quantitative parameter of spatial organization was $R>1$ in almost all fetal stages and $R<1$ in all adult stages (Fig. 7). When comparing the R values of all fetal vs. all adult stages, all comparisons were significant ($p<0.001$). Moreover, multiple significant differences were found between the fetal stages; all adult stages were significantly different from one another ($p<0.001$) except strings and double strings. Thus, the level of grouping was significantly different for the organizational stages illustrated in Fig. 1, which, in turn, validated the spatial distinctness of these stages.

## DISCUSSION

Whereas many anisotropic characteristics of AC are known[26], the SCSO in terms of the chondrocyte distribution beneath the AS is a ‘novel’ architectural characteristic of the tissue. Taking a broad approach, this study created the first model of human SCSO. Summarizing the changes during the lifetime of a hypothetical individual, our model revealed that the SCSO is neither congenital nor stable and that it undergoes complete destruction in OA. Thus, it revealed a surprisingly dynamic nature. We tested our model, which was based on assuming proliferation of OA-chondrocytes, by inducing proliferation specifically within early OA cartilage and monitoring the SCSO. We successfully recapitulated the destruction of SCSO *ex vivo* within the tissue, which confirmed our hypothesis and, thus, the soundness of our model. Quantitative analyses of the level of cellular grouping and statistical analyses unraveled significant differences between the reported organizational stages, which, in turn, validated the spatial distinctness of these stages. We demonstrated that the SCSO underwent destruction together with the chondrocyte-surrounding PCM. PCM destruction was detectable in *ex vivo* cartilages with severely impaired SCSO and, importantly, also in samples in which induced proliferation had intentionally destroyed the SCSO. Effectively, this established a novel *in vitro* methodology for studying SCSO and PCM destruction together over time, and within live tissue. Using this novel methodology, we clearly

demonstrated that loss of SCSO and collagenous PCM occur together and that both events are intertwined through proliferation specifically of early OA chondrocytes beneath the articular joint surface.

This study uncovered that the distinct SCSO and the PCM of human superficial chondrocytes are not congenital. It is important to mention that extensive and controlled data is available from animal models such as the rabbit and cow. The anisotropic adult AC evolves from an immature isotropic architecture by a synchronized postnatal process of tissue resorption and neoformation[27]. Maturational processes result in substantial differences between the superficial cell organizations of fetal, calf, and adult bovine cartilages[28, 29], and the most prominent changes in collagen architecture occur during postnatal development[30]. Differences between weight-bearing vs. non-weight-bearing areas of rabbit cartilage also exist, suggesting loading effects on the maturing cartilage architecture[31]. Thus, maturational changes in the SCSO described in Fig. 1 complement data derived from rabbit and cow models.

Research aimed at establishing a unified theory of the initial OA dysfunction so far was not successful[11]. However, next to others, proliferation is a well-established factor of OA-pathogenesis which occurs early in OA[7, 8]. The growth factor FGF-2 induces proliferation in intact and OA cartilage[32] and interacts[33, 34] with the three proliferation-associated signaling pathways of major importance in OA: Indian hedgehog, parathyroid hormone-related protein, and Wnt[35–37]. Thus, we chose FGF-2 as the obvious proliferation-inducing candidate and selected cartilage explants specifically containing strings and double strings as an image-based biomarker of early OA-affected organization[12, 16]. The here used method for visually classifying the organizational stage of chondrocyte groups was established previously[12, 16] but additional quantitative analyses and also a higher sample number would be helpful to confirm the presented results and their interpretation. FGF-2-induced proliferation led to SCSO loss, but none of these changes were visible in the controls. This demonstrated that proliferation was an underlying mechanism causing the induced SCSO loss and is possibly a mechanism responsible for *in situ* SCSO loss in OA. One should mention the possibility that the OA-related changes in SCSO reported for *ex vivo* cartilage could be due to cartilage erosion, exposing cell groupings that are typical of deeper zones. However, *in vitro* the FGF-2-induced SCSO loss was not associated with macroscopically apparent erosion. Previous studies have examined FGF-2 effects on chondrocytes, indicating age-dependent effects of cell proliferation and interactions with other growth factors[38, 39]. In calf cartilage, low-dose FGF-2 (3ng/ml) induced increased DNA content but higher concentrations did not. Here we used approximately 10pg/ml FGF-2, which was determined in[32]. Our study's proliferation-inducing FGF-2 concentration was well below the higher concentrations associated with proliferation inhibition[39]. Thus, no fundamental differences between FGF-2 protein application, used in[39], vs. transduction used here, were noted. Of course, such a comparison is difficult because the FGF-2 protein half-life is several hours[40] whereas FGF-2 can be expressed for at least 3 weeks via transduction[32]. Overall, this study is consistent with and builds upon the older studies, which did not examine cell organization. Moreover, our concentration was below 60pg/ml, the value measured in OA synovial fluid[41]; it is highly unlikely that the here reported events were based on non-physiogically high FGF-2 levels.

FGF-2 can emanate from the synovial fluid[42] and also from PCM damage[43]. Therefore, *in situ* FGF-2-mediated SCSO loss could originate from outside or inside the AC compartment and would theoretically interconnect cartilage pathology with other joint tissues, much in the sense of OA as a whole-organ-disease. Proliferation was mediated through FGF-2. Speculatively, other OA-relevant proliferation-inducing pathways would also lead to SCSO loss. However, there is yet no evidence.

Proliferation not only induced SCSO loss, it also affected the structural integrity of the PCM beneath the joint surface. This has important implications: the PCM consists of CollVI[44] and other components[45], which together with the enclosed cell form the "chondron"[46], a metabolic unit of AC[46], which acts as a mechano-sensitive cell-matrix interface[18, 19], protects the chondrocyte[17], and modulates its biosynthetic response [47]. In OA, changes in the chondron-related CollVI and proteoglycan distribution are followed by chondrocyte proliferation, pericellular microenvironment expansion, structural disruption, and chondrocyte clustering[48, 49]. Those changes affect the biomechanical signals perceived by the chondrocytes[18], explaining how PCM damage may contribute to OA-pathology. Here, we demonstrated that PCM changes were already detectable in double string chondrocytes prior to the cluster stage, and, thus, very early in OA. Structural disruption appeared to be associated with individual chondrocytes exiting or being released from their PCM, which we recorded using immuno-, auto-fluorescence and SHG-microscopy. The latter is a method for quantifying the intensity of micro-fibrillar collagens such as type I, II, III, V, XI. Thus, the documented PCM perforations affected some or all of those micro-fibrillar collagens. Using CollVI as immuno-marker, we demonstrated disintegration of the CollVI component around chondrocytes, which were diffusely arranged and had lost their SCSO. To the best of our knowledge, this extent of structural disintegration of the PCM has not been reported previously and is clearly relevant for OA-pathogenesis. First, CollVI contributes to chondrocyte survival by preventing apoptosis[17]. Secondly, an intact PCM prevents chondrocyte exposure to collagen type II fibrils. This keeps the discoidin domain receptor (DDR2) in a non-activated state and prevents metalloproteinase-13 enzyme and receptor expression[50]. Collectively, the here reported intertwined events of SCSO loss and PCM disintegration have the potential to affect chondrocyte survival, function, and phenotype. Further investigations of these important interactions will likely benefit from our novel *in vitro* methodology. This methodology consists of a) using spatially characterized cartilage explants and b) of induced chondrocyte proliferation in those explants, which replicates the process of loss of SCSO and PCM disintegration *in vitro*. Two potential applications come to mind. Given the well-known heterogeneity of OA chondrocytes, one could use cartilage explants with a defined SCSO that is stage-specific and, thus, standardized. Additionally, one could study the molecular, cellular, and structural aspects related to SCSO loss and PCM disintegration *in vitro* and test the effects of newly developed disease modifying OA drugs (DMOADs) on this induced advanced OA-like phenotype. The ability to induce a structural phenotype of human cartilage that is similar to advanced OA is novel and potentially of great significance and utility.

## Acknowledgments

We especially thank Klaus E. Kuettner, who initiated this work in Chicago in 2001, for his continuous friendship and encouragement during the entire project. We thank Frank Lichte and Miriam Linneweh for excellent technical assistance with scanning electron microscopy (F.L.) and multiphoton microscopy (M.L.). We are grateful for grants from the German Research Council (RO 2511/1-1, RO 2511/2-1, and AI 16/23 TPI FIII, INST 2388/30-1 FUGG), the German Social Accident Insurance (FR 0148 to B.R.), the Federal Ministry of Education and Research (REGiNA TP 2 to B.R., REGiNA TP 1 to W.K.A.), the National Institutes of Health (NIH; AR060331 to A.J.G.), for an intramural grant from the University of Tuebingen (fortüne to T.F), the Ministry of Science, Research and the Arts of Baden-Württemberg (33-729.55-3/214 and SI-BW 01222-91) and for the intramural support of the BG Trauma Clinic Tuebingen and the clinic operator Heidelberg Association for the Treatment of Occupational Injuries.

## References

1. Tuan RS, Chen AF, Klatt BA. Cartilage regeneration. J Am Acad Orthop Surg. 2013; 21:303–311. [PubMed: 23637149]
2. Kock L, van Donkelaar CC, Ito K. Tissue engineering of functional articular cartilage: the current status. Cell Tissue Res. 2012; 347:613–627. [PubMed: 22030892]
3. Roberts S, McCall IW, Darby AJ, Menage J, Evans H, Harrison PE, et al. Autologous chondrocyte implantation for cartilage repair: monitoring its success by magnetic resonance imaging and histology. Arthritis Res Ther. 2003; 5:R60–R73. [PubMed: 12716454]
4. Madry H, Luyten FP, Facchini A. Biological aspects of early osteoarthritis. Knee Surg Sports Traumatol Arthrosc. 2012; 20:407–422. [PubMed: 22009557]
5. Mitchell N, Lee ER, Shepard N. The clones of osteoarthritic cartilage. J Bone Joint Surg Br. 1992; 74:33–38. [PubMed: 1732261]
6. Andriacchi TP, Mundermann A, Smith RL, Alexander EJ, Dyrby CO, Koo S. A framework for the in vivo pathomechanics of osteoarthritis at the knee. Ann Biomed Eng. 2004; 32:447–457. [PubMed: 15095819]
7. Lotz MK, Otsuki S, Grogan SP, Sah R, Terkeltaub R, D'Lima D. Cartilage cell clusters. Arthritis and rheumatism. 2010; 62:2206–2218. [PubMed: 20506158]
8. Goldring MB. The role of the chondrocyte in osteoarthritis. Arthritis Rheum. 2000; 43:1916–1926. [PubMed: 11014341]
9. Schumacher BL, Su JL, Lindley KM, Kuettner KE, Cole AA. Horizontally oriented clusters of multiple chondrons in the superficial zone of ankle, but not knee articular cartilage. Anat Rec. 2002; 266:241–248. [PubMed: 11920387]
10. Chu CR, Williams AA, Coyle CH, Bowers ME. Early diagnosis to enable early treatment of pre-osteoarthritis. Arthritis Res Ther. 2012; 14:212. [PubMed: 22682469]
11. Bush JR, Beier F. TGF-beta and osteoarthritis--the good and the bad. Nat Med. 2013; 19:667–669. [PubMed: 23744142]
12. Aicher WK, Rolauffs B. The spatial organisation of joint surface chondrocytes: review of its potential roles in tissue functioning, disease and early, preclinical diagnosis of osteoarthritis. Ann Rheum Dis. 2014; 73:645–653. [PubMed: 24363359]
13. Rolauffs B, Williams JM, Grodzinsky AJ, Kuettner KE, Cole AA. Distinct horizontal patterns in the spatial organization of superficial zone chondrocytes of human joints. J Struct Biol. 2008; 162:335–344. [PubMed: 18325787]
14. Meinhardt M, Luck S, Martin P, Felka T, Aicher W, Rolauffs B, et al. Modeling chondrocyte patterns by elliptical cluster processes. J Struct Biol. 2012; 177:447–458. [PubMed: 22155191]
15. Rolauffs B, Rothdiener M, Bahrs C, Badke A, Weise K, Kuettner KE, et al. Onset of preclinical osteoarthritis: the angular spatial organization permits early diagnosis. Arthritis Rheum. 2011; 63:1637–1647. [PubMed: 21630246]
16. Rolauffs B, Williams JM, Aurich M, Grodzinsky AJ, Kuettner KE, Cole AA. Proliferative remodeling of the spatial organization of human superficial chondrocytes distant from focal early osteoarthritis. Arthritis Rheum. 2010; 62:489–498. [PubMed: 20112377]

17. Peters HC, Otto TJ, Enders JT, Jin W, Moed BR, Zhang Z. The protective role of the pericellular matrix in chondrocyte apoptosis. Tissue Eng Part A. 2011; 17:2017–2024. [PubMed: 21457093]
18. Guilak F, Alexopoulos LG, Upton ML, Youn I, Choi JB, Cao L, et al. The pericellular matrix as a transducer of biomechanical and biochemical signals in articular cartilage. Ann N Y Acad Sci. 2006; 1068:498–512. [PubMed: 16831947]
19. Kanbe K, Yang X, Wei L, Sun C, Chen Q. Pericellular matrilins regulate activation of chondrocytes by cyclic load-induced matrix deformation. J Bone Miner Res. 2007; 22:318–328. [PubMed: 17129169]
20. Seno M, Masago A, Nishimura A, Tada H, Kosaka M, Sasada R, et al. BALB/c 3Tcells co-expressing FGF-and soluble FGF receptor acquire tumorigenicity. Cytokine. 1998; 10:290–294. [PubMed: 9617574]
21. Cucchiarini M, Madry H, Ma C, Thurn T, Zurakowski D, Menger MD, et al. Improved tissue repair in articular cartilage defects in vivo by rAAV-mediated overexpression of human fibroblast growth factor 2. Mol Ther. 2005; 12:229–238. [PubMed: 16043094]
22. Cucchiarini M, Thurn T, Weimer A, Kohn D, Terwilliger EF, Madry H. Restoration of the extracellular matrix in human osteoarthritic articular cartilage by overexpression of the transcription factor SOX9. Arthritis Rheum. 2007; 56:158–167. [PubMed: 17195218]
23. Cucchiarini M, Ren XL, Perides G, Terwilliger EF. Selective gene expression in brain microglia mediated via adeno-associated virus type and type vectors. Gene Ther. 2003; 10:657–667. [PubMed: 12692594]
24. Samulski RJ, Chang LS, Shenk T. Helper-free stocks of recombinant adeno-associated viruses: normal integration does not require viral gene expression. J Virol. 1989; 63:3822–3828. [PubMed: 2547998]
25. Schenke-Layland K. Non-invasive multiphoton imaging of extracellular matrix structures. Journal of biophotonics. 2008; 1:451–462. [PubMed: 19343671]
26. Mow VC, Guo XE. Mechano-electrochemical properties of articular cartilage: their inhomogeneities and anisotropies. Annu Rev Biomed Eng. 2002; 4:175–209. [PubMed: 12117756]
27. Hunziker EB, Kapfinger E, Geiss J. The structural architecture of adult mammalian articular cartilage evolves by a synchronized process of tissue resorption and neoformation during postnatal development. Osteoarthritis Cartilage. 2007; 15:403–413. [PubMed: 17098451]
28. Jadin KD, Bae WC, Schumacher BL, Sah RL. Three-dimensional (3-D) imaging of chondrocytes in articular cartilage: growth-associated changes in cell organization. Biomaterials. 2007; 28:230–239. [PubMed: 16999994]
29. Jadin KD, Wong BL, Bae WC, Li KW, Williamson AK, Schumacher BL, et al. Depth-varying density and organization of chondrocytes in immature and mature bovine articular cartilage assessed by 3d imaging and analysis. J Histochem Cytochem. 2005; 53:1109–1119. [PubMed: 15879579]
30. Julkunen P, Iivarinen J, Brama PA, Arokoski J, Jurvelin JS, Helminen HJ. Maturation of collagen fibril network structure in tibial and femoral cartilage of rabbits. Osteoarthritis Cartilage. 2010; 18:406–415. [PubMed: 19941998]
31. Eggli PS, Hunziker EB, Schenk RK. Quantitation of structural features characterizing weight- and less-weight-bearing regions in articular cartilage: a stereological analysis of medial femoral condyles in young adult rabbits. Anat Rec. 1988; 222:217–227. [PubMed: 3213972]
32. Cucchiarini M, Terwilliger EF, Kohn D, Madry H. Remodelling of human osteoarthritic cartilage by FGF-2, alone or combined with Soxvia rAAV gene transfer. J Cell Mol Med. 2009; 13:2476–2488. [PubMed: 18705695]
33. Minina E, Kreschel C, Naski MC, Ornitz DM, Vortkamp A. Interaction of FGF, Ihh/Pthlh, and BMP signaling integrates chondrocyte proliferation and hypertrophic differentiation. Dev Cell. 2002; 3:439–449. [PubMed: 12361605]
34. Tuli R, Tuli S, Nandi S, Huang X, Manner PA, Hozack WJ, et al. Transforming growth factor-beta-mediated chondrogenesis of human mesenchymal progenitor cells involves N-cadherin and mitogen-activated protein kinase and Wnt signaling cross-talk. J Biol Chem. 2003; 278:41227–41236. [PubMed: 12893825]

35. Wu Q, Zhu M, Rosier RN, Zuscik MJ, O'Keefe RJ, Chen D. Beta-catenin, cartilage, and osteoarthritis. Ann N Y Acad Sci. 2010; 1192:344–350. [PubMed: 20392258]
36. Wang M, Shen J, Jin H, Im HJ, Sandy J, Chen D. Recent progress in understanding molecular mechanisms of cartilage degeneration during osteoarthritis. Ann N Y Acad Sci. 2011; 1240:61–69. [PubMed: 22172041]
37. Gomez-Barrena E, Sanchez-Pernaute O, Largo R, Calvo E, Esbrit P, Herrero-Beaumont G. Sequential changes of parathyroid hormone related protein (PTHrP) in articular cartilage during progression of inflammatory and degenerative arthritis. Ann Rheum Dis. 2004; 63:917–922. [PubMed: 15249318]
38. Shi S, Mercer S, Eckert GJ, Trippel SB. Growth factor regulation of growth factor production by multiple gene transfer to chondrocytes. Growth Factors. 2013; 31:32–38. [PubMed: 23302100]
39. Sah RL, Chen AC, Grodzinsky AJ, Trippel SB. Differential effects of bFGF and IGF-I on matrix metabolism in calf and adult bovine cartilage explants. Arch Biochem Biophys. 1994; 308:137–147. [PubMed: 8311446]
40. Shida J, Jingushi S, Izumi T, Iwaki A, Sugioka Y. Basic fibroblast growth factor stimulates articular cartilage enlargement in young rats in vivo. J Orthop Res. 1996; 14:265–272. [PubMed: 8648505]
41. Orito K, Koshino T, Saito T. Fibroblast growth factor in synovial fluid from an osteoarthritic knee with cartilage regeneration. J Orthop Sci. 2003; 8:294–300. [PubMed: 12768468]
42. Wang X, Manner PA, Horner A, Shum L, Tuan RS, Nuckolls GH. Regulation of MMP-expression by RUNXand FGFin osteoarthritic cartilage. Osteoarthritis Cartilage. 2004; 12:963–973. [PubMed: 15564063]
43. Vincent T, Hermansson M, Bolton M, Wait R, Saklatvala J. Basic FGF mediates an immediate response of articular cartilage to mechanical injury. Proc Natl Acad Sci U S A. 2002; 99:8259–8264. [PubMed: 12034879]
44. Poole CA, Ayad S, Gilbert RT. Chondrons from articular cartilage. V. Immunohistochemical evaluation of type VI collagen organisation in isolated chondrons by light, confocal and electron microscopy. J Cell Sci. 1992; 1(Pt 4):1101–1110. [PubMed: 1487492]
45. Zhang Z, Jin W, Beckett J, Otto T, Moed B. A proteomic approach for identification and localization of the pericellular components of chondrocytes. Histochem Cell Biol. 2011; 136:153–162. [PubMed: 21698479]
46. Poole CA. Articular cartilage chondrons: form, function and failure. J Anat. 1997; 1(Pt 1):1–13. [PubMed: 9279653]
47. Larson CM, Kelley SS, Blackwood AD, Banes AJ, Lee GM. Retention of the native chondrocyte pericellular matrix results in significantly improved matrix production. Matrix Biol. 2002; 21:349–359. [PubMed: 12128072]
48. Poole CA, Gilbert RT, Herbage D, Hartmann DJ. Immunolocalization of type IX collagen in normal and spontaneously osteoarthritic canine tibial cartilage and isolated chondrons. Osteoarthritis Cartilage. 1997; 5:191–204. [PubMed: 9219682]
49. Youn I, Choi JB, Cao L, Setton LA, Guilak F. Zonal variations in the three-dimensional morphology of the chondron measured in situ using confocal microscopy. Osteoarthritis Cartilage. 2006; 14:889–897. [PubMed: 16626979]
50. Xu L, Servais J, Polur I, Kim D, Lee PL, Chung K, et al. Attenuation of osteoarthritis progression by reduction of discoidin domain receptor in mice. Arthritis Rheum. 2010; 62:2736–2744. [PubMed: 20518074]

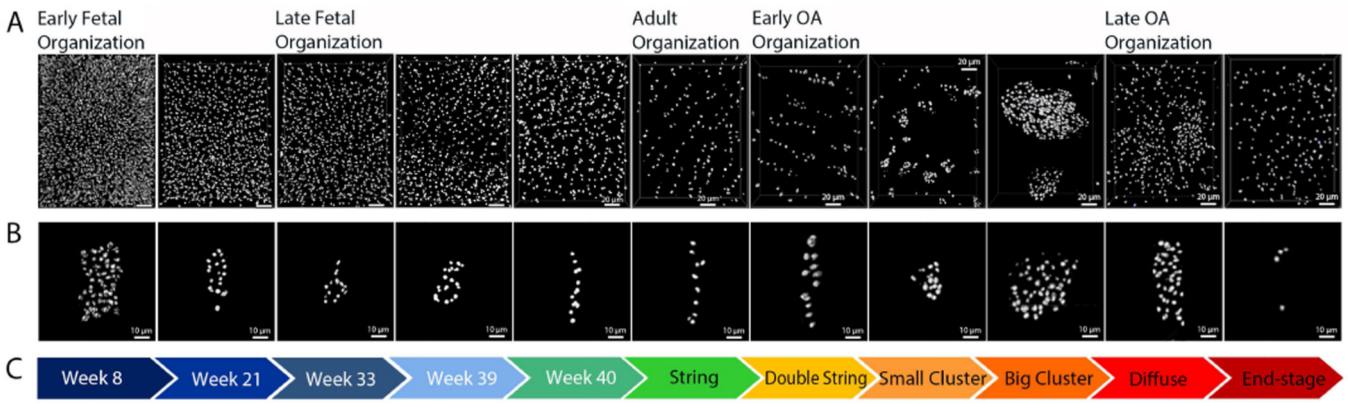


**Figure 1. Model of the spatial organization of human knee joint surface chondrocytes**

Representative images of propidium-iodide-stained chondrocyte nuclei in a top-down view onto the ASof human knee joint condyles (A) and selected patterns of spatial organization at a higher magnification (B) depict the sequence of typical stages of spatial organization that summarizes the lifetime of a hypothetical individual (C). The early fetal organization (gestational weeks 8–33) depicted no distinct organization. First precursors of the adult organization were visible at gestational week 40. In healthy adult cartilage, the spatial organization reached its peak with chondrocyte strings dominating the surface. In sequential order, OA-affected cartilages contained double strings, small and larger clusters, and the complete loss of any recognizable organization termed “diffuse”. The OA end-stage consisted of areas of low cellularity. Number of fetal knee joints: $8^{th}$ week of gestation: n=3 individuals, $21^{th}$ week: n=1, $33^{th}$ week: n=1, $39^{th}$ week: n=1, $40^{th}$ week: n=1; number of intact donor knee joints and donors: n=4, number of patient knee joints and patients: n=6. Number of images analyzed: 8th week: n=6, 21th week: n=4, 33th week: n=3, 39th week: n=3, 40th week: n=3; number of adult images: strings: n=6, double strings: n=6, cluster: n=5, diffuse: n=6.

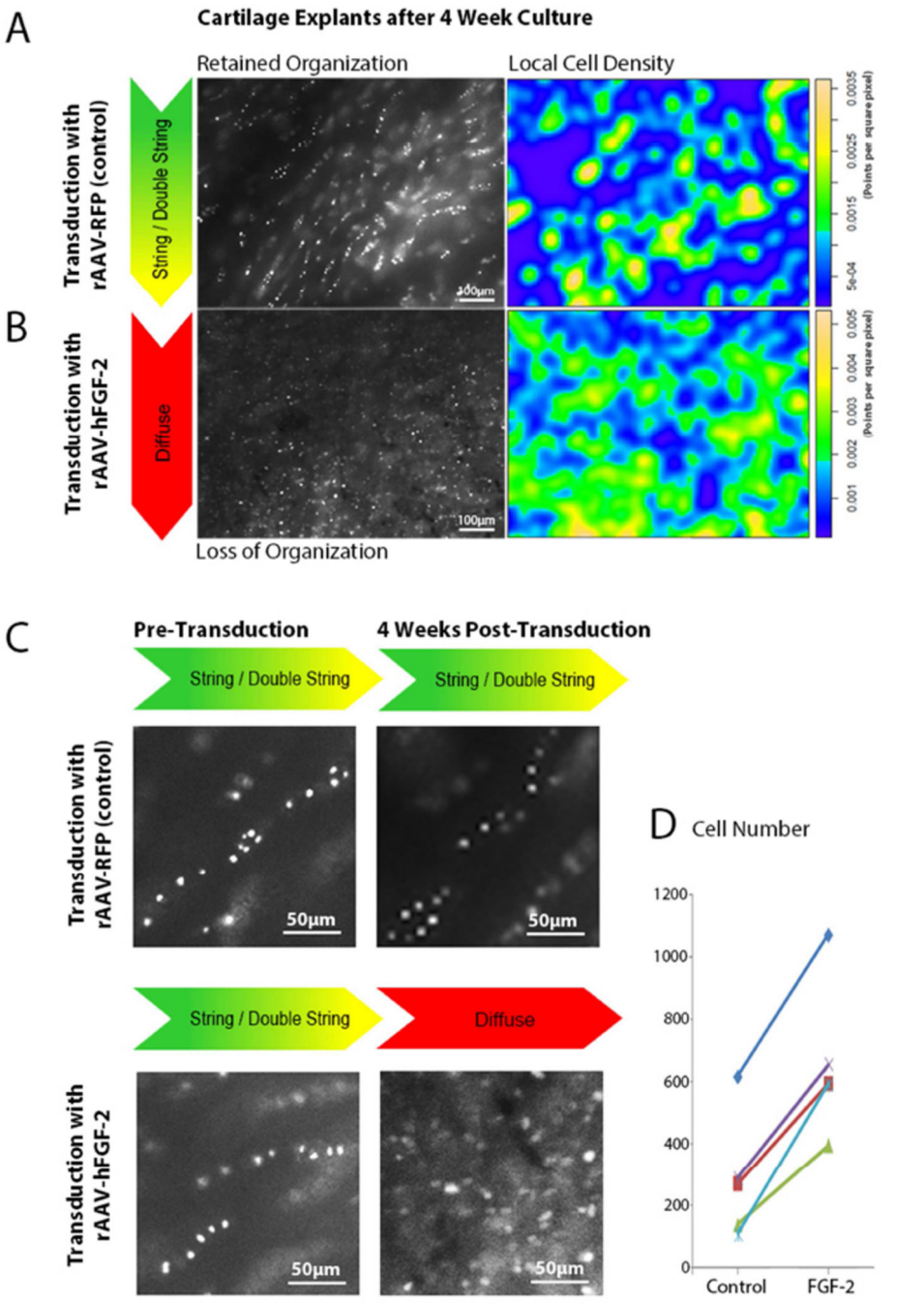


**Figure 2. Loss of spatial organization can be recapitulated by FGF-2 transduction-induced proliferation of string and double string chondrocytes within the articular surface of early OA cartilage explants**

Depicted are chondrocyte nuclei in a top-down view onto the articular surface (A,B,C). A represents the spatial organization of control surfaces transduced with rAAV-RFP, which contained double strings and a few strings after 4 weeks culture. B illustrates rAAV-hFGF-2-transduced chondrocytes after 4 weeks culture. Those chondrocytes had lost any recognizable spatial organization and their arrangement was comparable to the diffuse stage of late OA (see Fig. 1A). The loss of organization had occurred in articular surfaces together

with a relative increase in the local cell density over control surfaces, depicted as color-coded local cell density maps (A,B). Pre-transduced articular surfaces containing string and double string chondrocytes and representative chondrocyte groups 4 weeks after transduction with rAAV-RFP or rAAV-hFGF-2 are depicted in (C). rAAV-hFGF-2-transduced samples contained higher chondrocyte numbers over controls (D; $p<0.05$), indicating that FGF-2 transduction had induced proliferation. Number of patient knee joints, patients, and individually performed experiments: n=6. Normality was tested with the Kolmogorov-Smirnov-Test, which indicated not normally distributed data. Statistical differences were determined by the Mann-Whitney-Rank-Sum-Test. Differences were considered statistically significant at $p<0.05$.

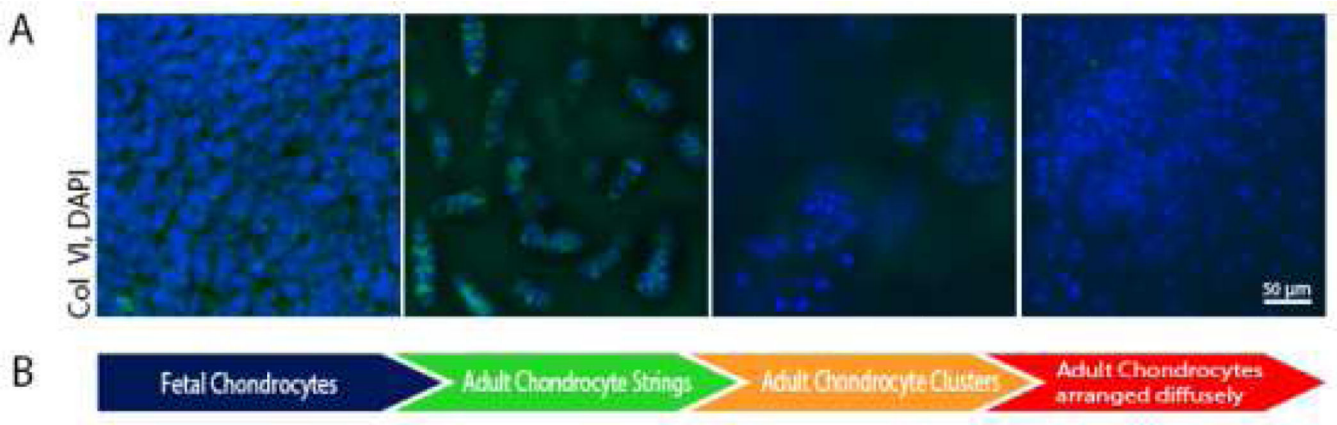


**Figure 3. Impairment of both the spatial organization and the chondrocyte-surrounding pericellular matrix in the articular surfaces of ex vivo cartilage samples, assessed by fluorescence microscopy**

Depicted are fluorescence microscopy images of DAPI-stained chondrocyte nuclei (blue) and the collagen type VI (green) stained PCM (A) and the associated stages of spatial organization (B). The collagen type VI PCM component was not present around fetal chondrocytes but fully present around adult chondrocyte strings representing mature intact tissue. Little or no collagen type VI signal was detectable around adult chondrocyte clusters representing a spatial stage within OA tissue. Collagen type VI was not detectable in the diffuse stage of spatial organization. Number of knee joints for samples for histological analyses: n=4 (fetal), n=6 (adult).

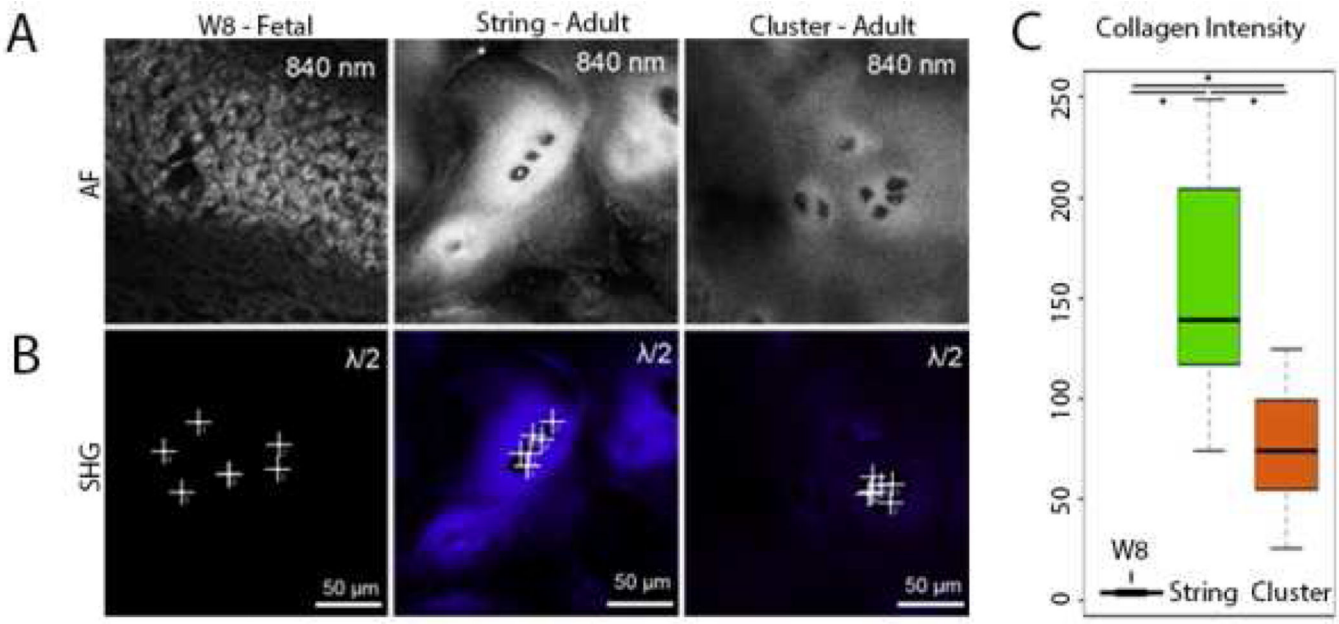


**Figure 4. Impairment of both the spatial organization and the chondrocyte-surrounding pericellular matrix, assessed by second harmonic generation multiphoton microscopy (SHG)**

Multiphoton-induced autofluorescence (AF) was used to localize chondrocytes of interest beneath the articular joint surface of cartilage explants from the knee joint condyles (A). SHG microscopy (B) revealed that micro-fibrillar collagen components of the PCM were not detectable around fetal chondrocytes (W8: week 8), present around adult string chondrocytes, and that little micro-fibrillar collagen components were detectable in the PCM of adult cluster chondrocytes representing a spatial stage within OA tissue. SHG quantification of micro-fibrillar collagens (C) was performed at locations indicated with + in B. The resulting micro-fibrillar collagen intensity (C) revealed significant differences in the intensities between fetal, string, and cluster chondrocytes. These are marked with * and black lines. Number of knee joints for samples for SHG quantification: n=3 (fetal), n=3 (adult). Normality was tested with the Kolmogorov-Smirnov-Test, which indicated not normally distributed data. Statistical differences were determined by the Kruskal-Wallis One Way Analysis of Variance on Ranks. The contrasts between the different micro-fibrillar collagen intensities were tested with the post hoc Tukey Test. Differences were considered statistically significant at $p<0.05$.

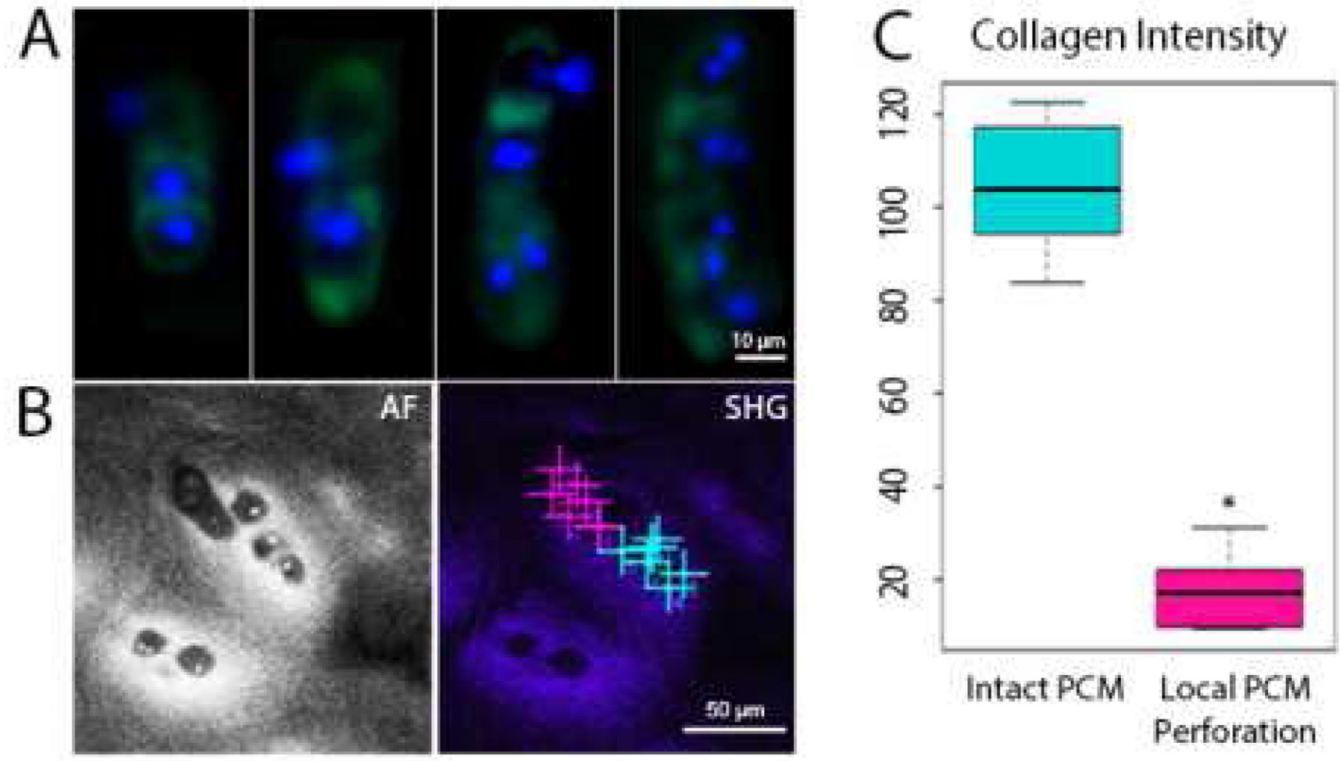


**Figure 5. Localized PCM perforations with individual chondrocytes exiting or being released from the PCM visualized by fluorescence microscopy and quantified by second harmonic generation multiphoton microscopy (SHG)**

Depicted are fluorescence microscopy images of DAPI-stained chondrocyte nuclei (blue) and the collagen type VI (green) stained PCM (A). Individual chondrocytes are localized within gaps of the PCM or are clearly localized outside the PCM boundary, indicating that chondrocytes are exiting or being released from their PCM. Using AF, such PCM perforations were clearly visible (B). SHG quantification of micro-fibrillar collagens (C) was performed at locations representative for intact appearing PCM areas indicated with + (light blue) in B and at locations representative for perforated PCM areas indicated with + (dark pink) in B. Quantitative SHG revealed that distinct perforations were characterized by a significantly lower micro-fibrillar collagen intensity than intact areas of the same PCM (C). Number of knee joints for fluorescence microscopy: n=5, number of knee joints for SHG quantification: n=3. Normality was confirmed with the Kolmogorov-Smirnov-Test. Statistical differences were determined by the Student t-test. Differences were considered statistically significant at $p<0.05$.

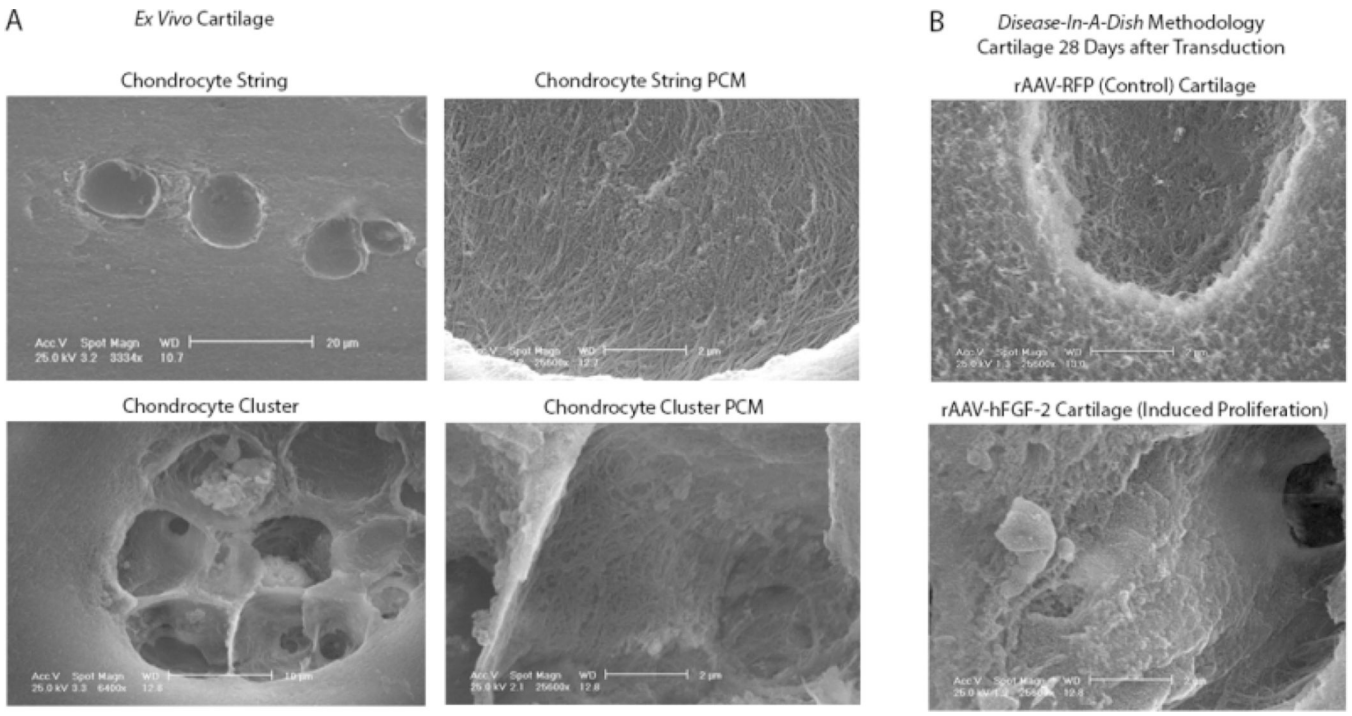


**Figure 6. Scanning electron images (SEM) in a top-down view onto the chondrocyte-surrounding pericellular matrix beneath the articular surface of human ex vivo cartilage and cartilage subjected to induced proliferation in the context of our novel in vitro methodology**

Depicted are representative SEM images of adult chondrocyte strings and OA-associated clusters in an overview and their PCM at higher magnification (A). These images illustrate a PCM network of interwoven fibers around chondrocytes arranged in strings, whereas this PCM network was less apparent around clustered chondrocytes. In those, the cell-matrix interface was irregularly shaped and broken up. In B, SEM images depict chondrocytes 28 days after they were subjected to transduction with FGF-2 to induce proliferation or with RFP as controls. The PCM fiber network was intact in control samples but was absent around FGF-2-transduced chondrocytes, which had proliferated and lost their spatial organization. Those chondrocytes were surrounded by a broken-up, deformed cell matrix interface. Scale bar, 20μm (left images, top and bottom row). Scale bar, 2μm (all other images). Number of knee joints: n=4 (*ex vivo*), n=3 (*in vitro*).

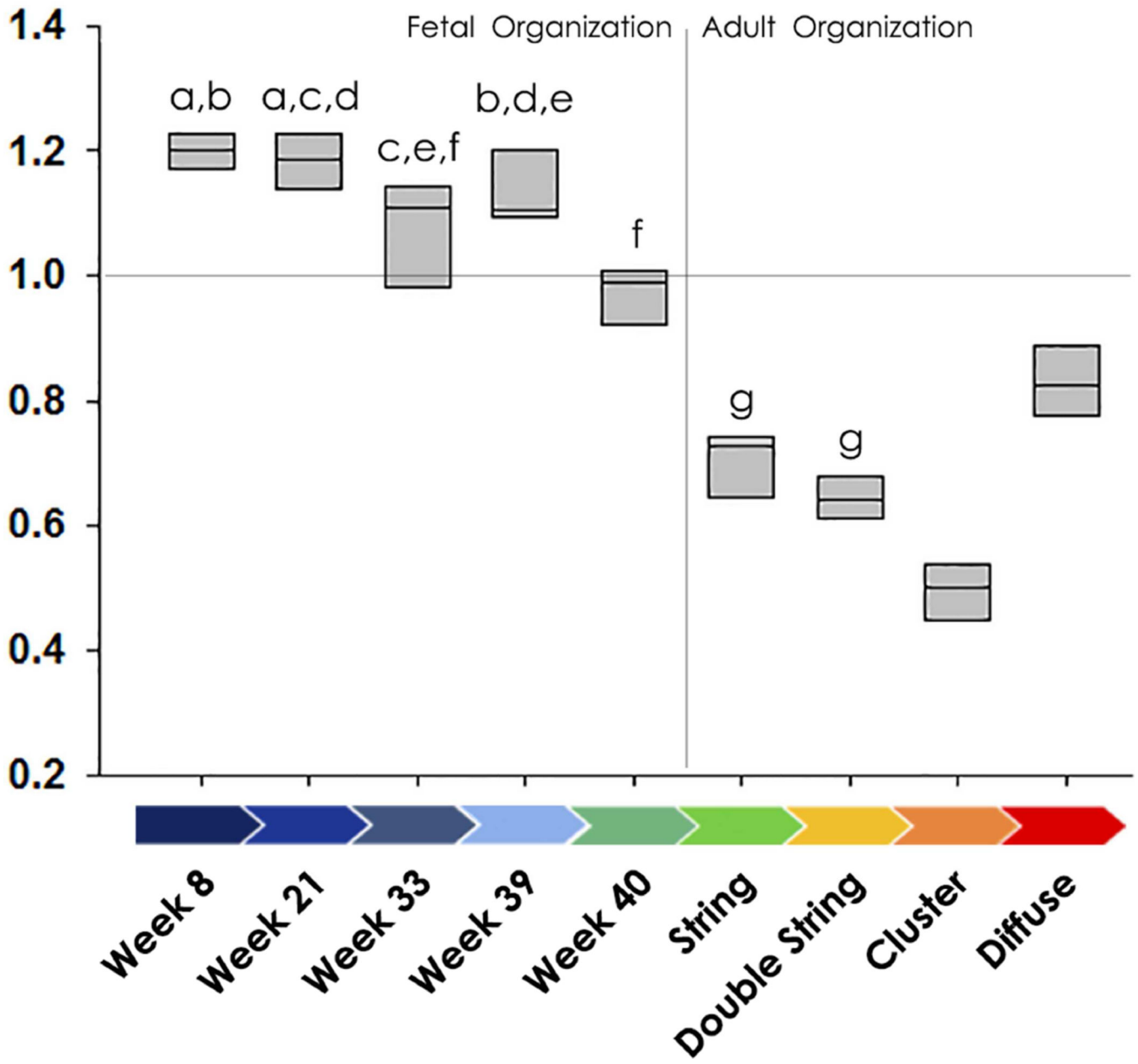


**Figure 7. Clark-Evans-Aggregation-Index (R) describing the presence or absence of cellular grouping as quantitative parameter of spatial organization**

Depicted are the values for the Aggregation-Index (R), which is calculated from the distance of each chondrocyte to its nearest neighbor. Briefly, R<1 describes a grouped organization, R>1 a homogeneous organization, and R=1 a random organization, indicated with a grey reference line at y=1.0. When statistically comparing each group with all other groups using the Holm-Sidak post-hoc test, 29 pairwise comparisons of the 36 possible comparisons were significant. 7 pairwise comparisons did not reach significance and are indicated with small letters, e. g. “a” indicates that the comparison between “Week 8” and “Week 21” was not significant whereas all other comparisons of “Week 8” with “Weeks 21–40” and with the “Adult Organization” were significant. Generally, the fetal spatial organization except

"Week 40" was characterized by a homogeneous organization whereas the R values of the adult organization were significantly different, indicating cellular grouping. The organizational pattern of strings typical for healthy cartilage was significantly different from the grouping of clustered and diffusely arranged chondrocytes typical for OA. Moreover, the organizational pattern of double strings as marker of early OA-affected organization was significantly different from the later stages of OA organization.